Multi-Phase Winding with In-Conductor Direct Cooling Capability for a 48 V Traction Drive Design

Stefan Haller[1], *Student Member, IEEE*, Johan Persson[2], Peng Cheng[1] and Kent Bertilsson[1]

***Abstract*—Traction drive applications demand high power density motors with a good stator cooling design. We propose a novel multi-phase winding for a 48 V traction drive design having identical preformed hollow copper conductors with in-conductor direct cooling capability. This paper studies the cooling performance of an individual conductor phase using either EGW50/50 or water as coolant. Analytical calculations and experiments are conducted on a straight conductor of the same length using 20 °C water as coolant. The results are then cross verified with those from the FEM simulations to validate the simulation setup. Then a final simulation is conducted at a current of 700 A and a current density of 49.5 A/mm^2 on the preformed conductor using 65 °C EGW50/50 as coolant at a pressure of 140 kPa. The results highlight the exceptional performance of the cooling design which enables a power dissipation of 710 W at a maximum conductor temperature rise of only 56.9 °C.**

***Index Terms*—In-conductor direct cooling, hollow conductor, multi-phase winding, electrical machine, traction drive, low-voltage, 48V**

I. Introduction

To increase the power density of traction drives, different cooling methods can be used. Conventionally, heat from the stator of a motor is extracted either by cooling jackets in its housing, or by boreholes in the steel pack or beside the air-gap. For high-power traction drives, oil cooling inside the motor housing and liquid cooling inside the rotor shaft are also used. For high voltage motor designs, direct conductor oil cooling has been investigated in [1], [2] and [3]. Lindh et al. [4] utilized water in steel tube at the center of litz wire for its winding cooling. Patzak et al. [5] showed a low voltage induction motor design called ISCAD which used a novel half squirrel cage winding design having a liquid cooled end ring. In [6], the thesis investigated an air-cooled hollow conductor, both in simulation and in experiment. In [7] and [8], slot cooling with ethylene glycol water 50/50 (EGW50/50) through tubes are used for enhanced cooling of the winding in the slot. The major difference between these referenced publications and this work is, the usage of direct cooling through the conductor center of the entire winding. The 48 V low-voltage design allows the use of water or EGW50/50 and hence has the potential to achieve a better motor winding cooling result.

Financial support of the project "48 V powertrain FFI concept study" by the Swedish Energy Agency is gratefully acknowledged.

[1]S, Haller, P. Cheng and K. Bertilsson are with the Department of Electronics Design, Mid Sweden University, Sundsvall, Sweden (e-mail: stefan.haller@miun.se, peng.cheng@miun.se, kent.bertilsson@miun.se).

[2]J. Persson is with the Department of Natural Sciences, Mid Sweden University, Sundsvall, Sweden (e-mail: johan.persson@miun.se).

In all traction drives, the major fraction of the heat during high load conditions is generated at the machine's stator winding. The power density of the motor is typically limited by the maximum hot spot temperature of the insulation coating in the center of the winding. High winding temperatures can also reduce the partial load efficiency of the traction drive, which will translate to a reduced range for electric vehicles (EVs). As shown in [9], range rating is a primary parameter to optimize for EV applications. Thus, a good cooling design is very important for both, the performance and the efficiency of traction drives in EV applications.

In this paper, we propose a multi-phase star-topology winding for a 48 V traction drive design, which incorporates in-conductor direct cooling capability to extract the heat directly from where most of it is generated. The paper studies the cooling performance of an individual conductor phase, of which is used in 48 identical copies to form the winding. Analytical calculations and FEM simulations are conducted, using either water or EGW50/50 as coolant. Measurements on two versions of the coil conductor, using water, are also performed on a lab setup to verify the results.

II. Winding Design

The 48 V traction motor design, which is a 48-slot 8-pole permanent magnet assisted synchronized reluctance motor, has a steel pack outer diameter of 225 mm and an active length of 150 mm. It uses a 48-phase star-topology distributed winding made with 48 identical preformed hollow copper conductors as shown in Fig. 1. The hollow conductor is used in order to incorporate in-conductor direct cooling capability, so that coolant can flow through each individual phase to effectively dissipate the heat generated from the load current. The copper conductor has an outer diameter of 4.5 mm and an inner diameter of 1.5 mm, with a length of about 950 mm. The inner hole takes 11.1 % of the cross-sectional area of the conductor, resulting in a copper area of about 14.14 mm^2. The increased DC resistance due to the center opening can be compensated by the reduced conductor temperature due to improved cooling. Since the skin-effect pushes the AC current towards the outer surface, the center opening has a minor effect on the additional AC loss. The 48-phase winding is designed to have all phases in a parallel hydraulic circuit. Therefore, the coolant pressure drop is the same across all phases and the total coolant flow rate is 48 times as that of the individual phase. The first prototype assembly of this winding design into a 3D printed stator mold is shown in Fig. 2. With this 48 V low-voltage design, it is now possible to use coolants of better

978-1-7281-9944-3/20/$31.00 ©2020 IEEE

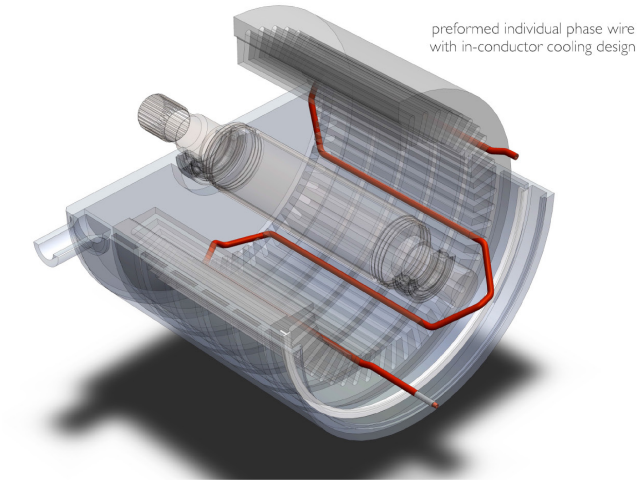

Fig. 1. Single phase coil with in-conductor cooling design inside the slot.

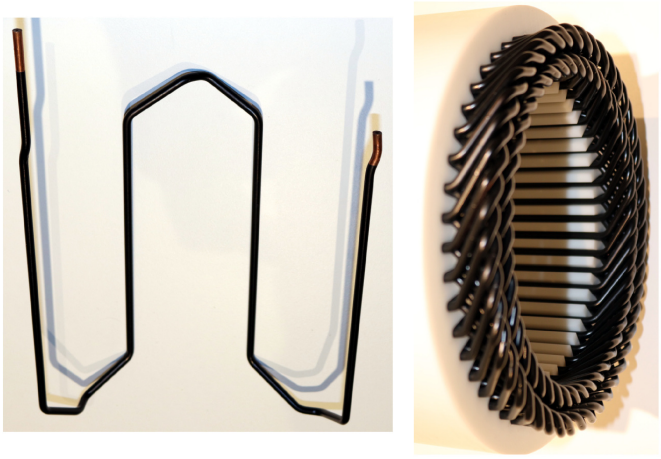

Fig. 2. The W-shaped coil prototype to the left and the end-winding assembly to the right.

thermal performance, such as EGW50/50, and let them directly contact the copper conductor surface. Both of these features are impossible in conventional high-voltage motor designs that use oil-based coolants and require insulation coating on the conductors. These important features from the low-voltage design should be further exploited in order to demonstrate the inherent cooling performance advantage of the low-voltage traction motor design compared to state-of-the-art high-voltage drives.

III. Analytical Calculations

This section provides a simple analytical study for the water-based in-conductor direct cooling to deduce the operating condition of the copper conductor. In order to simplify the calculations, the study assumes a thermal equilibrium state with a constant coolant flow rate at $0.3\,\mathrm{l/min}$ and a DC current of $520\,\mathrm{A}$ through the conductor. Water of $20\,^{\circ}\mathrm{C}$ is assumed at the coolant inlet. The study assumes a linear thermal gradient through the conductor and focuses on estimating the coolant heat transfer coefficients at both inlet and outlet of the conductor in order to deduce the averaged results. For $20\,^{\circ}\mathrm{C}$ water at the inlet of the conductor, the parameters in Table I are used.

TABLE I
20°C Water Coolant Parameter Constants Used for the Analytical Calculations [10].

Symbol	Description	
ρ	Density	$997.78\,\mathrm{kg/m^3}$
v	Kinematic viscosity	$9.7937 \times 10^{-7}\,\mathrm{m^2/s}$
λ	Heat conductivity	$0.604\,75\,\mathrm{W/(m\,K)}$
$C_{p,v}$	Volumetric heat capacity	$4.067\,\mathrm{J/(cm^3\,K)}$
P_r	Prandtl number	6.5870

For the copper conductor of $950\,\mathrm{mm}$ length and $1.5\,\mathrm{mm}$ of inner diameter using $20\,^{\circ}\mathrm{C}$ water as the coolant with a flow rate Q of $0.3\,\mathrm{l/min}$, the Reynolds number Re is:

$$\begin{aligned} Re &= u \cdot \frac{D}{v} = \frac{Q}{A} \cdot \frac{D}{v} \\ &= \frac{5 \times 10^{-6}\,\mathrm{m^3/s}}{\pi \cdot (0.75 \times 10^{-3}\,\mathrm{m})^2} \cdot \frac{1.5 \times 10^{-3}\,\mathrm{m}}{9.7937 \times 10^{-7}\,\mathrm{m^2/s}} \\ &\approx 4333.53 \end{aligned} \tag{1}$$

with u being the flow speed in meter per second, Q the flow rate in cubic meters per second, A the conductors inner area in square meter, D the conductor inner diameter in meter and v the kinematic viscosity in square meter per second.

The flow is assumed to be turbulent as its Reynolds number is larger than 4000. Then the pressure drop Δp across the conductor can be calculated by the Darcy–Weisbach equation:

$$\begin{aligned} \Delta p &= L \cdot f_D \cdot \frac{\rho}{2} \cdot \frac{u^2}{D} = L \cdot f_D \cdot \frac{\rho}{2} \cdot \frac{(\frac{Q}{A})^2}{D} \\ &= 0.95\,\mathrm{m} \cdot 0.0404 \cdot \frac{997.78\,\mathrm{kg/m^3}}{2} \cdot \frac{(2.83\,\mathrm{m/s})^2}{1.5 \times 10^{-3}\,\mathrm{m}} \\ &\approx 102.2\,\mathrm{kPa} \end{aligned} \tag{2}$$

with Δp as pressure drop in pascal, L as length of the conductor in meter, f_D as Darcy friction factor and ρ as coolant density in kilogram per cubic meter.

The Darcy friction factor for the smooth pipe can be calculated by employing the Petukhov correlation:

$$\begin{aligned} f_D &= (0.79 \cdot \ln(Re) - 1.64)^{-2} \\ &= (0.79 \cdot \ln(4333.53) - 1.64)^{-2} \\ &\approx 0.0404. \end{aligned} \tag{3}$$

Now the heat transfer function of the pipe is calculated by obtaining the Nusselt number Nu for turbulent flow using the Gnielinski correlation:

$$\begin{aligned} Nu &= \frac{Pr \cdot (f_D/8) \cdot (Re - 1000)}{12.7 \cdot \sqrt{f_D/8} \cdot (Pr^{2/3} - 1) + 1} \\ &= \frac{6.5870 \cdot (0.0404/8) \cdot (4333.53 - 1000)}{12.7 \cdot \sqrt{0.0404/8} \cdot (6.5870^{2/3} - 1) + 1} \\ &\approx 24.28275 \end{aligned} \tag{4}$$

with Pr as Prandtl number.

Finally, the heat transfer coefficient h is calculated as

$$\begin{aligned} h &= Nu \cdot \frac{\lambda}{D} \\ &= 24.28275 \cdot \frac{0.604\,75\,\mathrm{W/(m\,K)}}{1.5 \times 10^{-3}\,\mathrm{m}} \\ &\approx 9790\,\mathrm{W/(m^2K)} \end{aligned} \tag{5}$$

with λ as thermal conductivity of the coolant in watt per meter kelvin.

Resulting in a heat transfer factor h_p for the $950\,\mathrm{mm}$ long conductor with an inner surface area A_i of $44.7\,\mathrm{cm^2}$ of

$$\begin{aligned} h_p &= A_i \cdot h \\ &= 44.7 \times 10^{-4}\,\mathrm{m^2} \cdot 9790\,\mathrm{W/(m^2K)} \\ &\approx 43.83\,\mathrm{W/K}. \end{aligned} \tag{6}$$

Now, the conductor inlet temperature needs to be estimated using this coolant heat transfer coefficient of $43.83\,\mathrm{W/K}$ and an iterative approach until it converges to a number that is higher than the coolant inlet temperature of $20\,^\circ\mathrm{C}$. As for the starting point of the iteration, the DC resistance of the $950\,\mathrm{mm}$ long copper conductor at $20\,^\circ\mathrm{C}$ is about $1.129\,\mathrm{m\Omega}$, and it has a temperature coefficient of $0.004/\mathrm{K}$. So at $520\,\mathrm{A}$, its loss is about $305.28\,\mathrm{W}$. The following is the results of five iterations.

$$\begin{aligned} 305.28/43.83 &\approx 6.9651 \\ (1 + 0.004 \cdot 6.9651) \cdot 305.28/43.83 &\approx 7.1591 \\ (1 + 0.004 \cdot 7.1591) \cdot 305.28/43.83 &\approx 7.1645 \\ (1 + 0.004 \cdot 7.1645) \cdot 305.28/43.83 &\approx 7.1647 \\ (1 + 0.004 \cdot 7.1647) \cdot 305.28/43.83 &\approx 7.1647 \end{aligned}$$

It converged at ΔT_{start} of $7.16\,^\circ\mathrm{C}$ which is the temperature difference between coolant and conductor. So the estimated conductor inlet temperature is $27.16\,^\circ\mathrm{C}$.

To estimate the coolant outlet temperature conservatively, first the same coolant heat transfer coefficient of $43.83\,\mathrm{W/K}$ and ΔT_{start} of $7.16\,^\circ\mathrm{C}$ at the outlet is assumed, even though the real coefficient will be higher and ΔT_{end} will be lower as the viscosity is reduced when the water heats up. The coolant's volumetric heat capacity $C_{p,v}$ is assumed to about $4.067\,\mathrm{J/(cm^3\,K)}$ and the constant flow rate to $0.3\,\mathrm{l/min}$. The following is the results of five iterations.

$$\begin{aligned} (1 + 0.004 \cdot 7.1647) \cdot 305.28/(4.067 \cdot 5) &\approx 15.4428 \\ (1 + 0.004 \cdot (7.1647 + 15.4428/2)) \cdot \frac{305.28}{(4.067 \cdot 5)} &\approx 15.9065 \\ (1 + 0.004 \cdot (7.1647 + 15.9065/2)) \cdot \frac{305.28}{(4.067 \cdot 5)} &\approx 15.9204 \\ (1 + 0.004 \cdot (7.1647 + 15.9204/2)) \cdot \frac{305.28}{(4.067 \cdot 5)} &\approx 15.9208 \\ (1 + 0.004 \cdot (7.1647 + 15.9208/2)) \cdot \frac{305.28}{(4.067 \cdot 5)} &\approx 15.9208 \end{aligned}$$

Resulting in a conservative estimate of the coolants outlet temperature of $35.92\,^\circ\mathrm{C}$ for $20\,^\circ\mathrm{C}$ inlet.

For water of $35.92\,^\circ\mathrm{C}$ at the outlet of the conductor, the parameters provided in Table II are used.

TABLE II
35.92°C WATER COOLANT PARAMETER CONSTANTS USED FOR THE ANALYTICAL CALCULATIONS [10].

Symbol	Description	
ρ	Density	$993.27\,\mathrm{kg/m^3}$
v	Kinematic viscosity	$6.9245 \times 10^{-7}\,\mathrm{m^2/s}$
λ	Heat conductivity	$0.627\,33\,\mathrm{W/(m\,K)}$
$C_{p,v}$	Volumetric heat capacity	$4.041\,\mathrm{J/(cm^3\,K)}$
P_r	Prandtl number	4.4603

Taking similar calculations, by using Eq. 1 – Eq. 6 and the parameters from Table II, the following results are derived:

$$\begin{aligned} Re &\approx 6129.15 \\ \Delta p &\approx 91.4kPa \\ f_D &\approx 0.0363 \\ Nu &\approx 34.36634 \\ h &\approx 14373W/(m2 * K) \\ h_p &\approx 64.25W/K \end{aligned}$$

Finally, the conductor outlet temperature is estimated using a similar approach as of the conductor's inlet temperature, which yields a ΔT_{end} of $5.15\,^\circ\mathrm{C}$. So the estimated conductor end temperature is the coolant outlet temperature plus ΔT_{end} of $5.15\,^\circ\mathrm{C}$ to reach $41.07\,^\circ\mathrm{C}$.

IV. FEM/CFD Simulation Setup

The simulation is subdivided into two stages, first, the model is evaluated with the same parameters as in the analytical model to validate the model and show mesh independence, then the W-shaped conductor in Fig. 2 is tested with $65\,^\circ\mathrm{C}$ coolant EGW50/50 [10] with a mesh which is finer than the finest from the independence study. The simulation is a multi-physics coupled model with the electric current, k-ε turbulent flow with wall function, and heat conduction. Heat is transported with the fluid (convection) and the electric current heats the copper by Joule heating, in turn, the change in temperature alters the material properties. The system is solved by iterations until a stable solution is found. All simulations are performed in Comsol Multiphysics 5.3a [11].

As boundary conditions for the straight conductor, the inlet side has a nominal current of $520\,\mathrm{A}$ in the conductor-wall and $20\,^\circ\mathrm{C}$ water is added with a 18–$100\,\mathrm{kPa}$ pressure drop Δp over the conductor. All material parameters except that of the coolant are taken from the standard materials library in Comsol. The coolant parameters density, kinematic viscosity, and specific heat are approximated by a third degree polynomial functions of temperature in the region $20\,^\circ\mathrm{C}$ to $107\,^\circ\mathrm{C}$. The W-shaped conductor is represented by ten times as many elements as the straight conductor in order to resolve the bends properly. The boundary conditions are then the inlet side has a nominal current of $700\,\mathrm{A}$ in the conductor-wall and $65\,^\circ\mathrm{C}$ EGW50/50 is added with a $140\,\mathrm{kPa}$ pressure drop over the conductor. The electrical pump power $\dot{W}$ to achieve the required pressure and flow is calculated with

$$\dot{W} = 2 \cdot Q \cdot \Delta p. \tag{7}$$

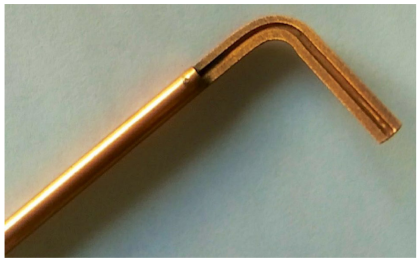

Fig. 3. Cut of the hollow conductor, showing that a 90° bend has no major impact on the inner diameter.

The factor 2, to estimate the required electrical pump power, is used which is appropriate according to [12]. This results in about 1.4 W for a single conductor with EGW50/50 at 140 kPa pressure drop and assuming a flow rate Q of about 0.3 l/min.

V. Measurement Setup

To verify the analytical and simulation model, a customized hollow conductor has been fabricated in two versions. A straight version with no bends, and a W-shaped one which forms one of the 48 stator coils of the machine shown in Fig. 2. Both conductors use the same material and dimensions. To confirm that the bends do not have a major impact on the conductors inner diameter, a cross-sectional cut at a 90° bend was made, shown in Fig. 3.

For the heat transfer and flow rate measurements, the experimental setup shown in Fig. 4 was used. For these initial measurements, a chiller keeps the coolant constantly at 20 °C at the conductors inlet. To ensure a constant pressure at the conductors coolant inlet, a set of adjustable pumps is used. To minimize pressure ripple, an air filled expansion vessel is connected between the pump and the conductors coolant inlet. To reduce convection and thermal radiation losses, the conductor is covered with a 7.5 mm thick insulation material with a thermal conductivity $\lambda \leq 0.033\,\mathrm{W/(m \cdot K)}$.

The measurement setup provides constant pressure in the range of 20 kPa to 100 kPa. Fig. 5 shows the flow diagram of the coolant, including pressure, flow, and temperature measurement points. The coolant temperature at the inlet and outlet as well as the conductor temperature at the start and the end is measured. Table III shows the location of the temperature sensors.

TABLE III
Location of Temperature Sensors.

Sensor	Location
TP 1	Conductor start
TP 2	Conductor end
TP 3	Coolant inlet
TP 4	Coolant outlet

A pair of 20 mm wide solid copper clamps are used to connect the conductor to an adjustable DC source. Conductor and clamp surface are untreated bare copper. The nominal

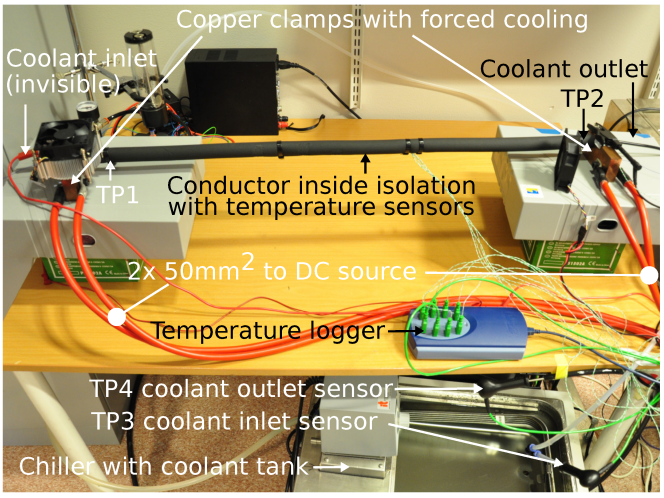

Fig. 4. Experimental setup with the straight version of the conductor mounted in the copper clamps to the left and right. The conductor temperature is measured at points TP 1 and TP 2.

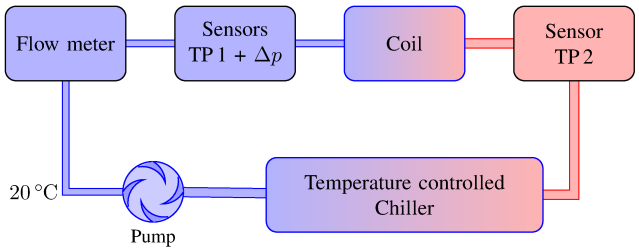

Fig. 5. Measurement setups schematic coolant flow diagram through the conductor with chiller and pump on the bottom and flow, pressure and temperature measurement on the top.

resistance of the 950 mm long conductor with an effective copper area of 14.14 mm² at 20 °C is 1.129 mΩ. To calculate the contact resistance, the differential clamp voltage ΔU was measured. With a conductor current I_c of 520 A across the conductor, ΔU is 702 mV, resulting in a contact resistance R_{cc} of

$$\begin{aligned} R_{cc} &= \frac{1}{2} \cdot \left(\frac{U}{I} - R_c\right) \\ &= \frac{1}{2} \cdot \left(\frac{0.702\,\mathrm{V}}{520\,\mathrm{A}} - 1.129\,\mathrm{m\Omega} \cdot 1.0616\right) \\ &\approx 0.076\,\mathrm{m\Omega} \end{aligned} \tag{8}$$

on each clamp. The factor 1.0616 is the estimated temperature coefficient due to copper heating.

The connection from clamp to DC source is made by two parallel connected 50 mm² cables at each clamp, as illustrated in Fig. 4. Both clamps are forced air cooled to reduce the influence of the heating from the feeding cables and their contacts. The cold side, to the left, has an additional heat-sink mounted to keep the clamp at ambient temperature which is approximately the coolants temperature at this clamp.

Even though measures have been taken to reduce the effect of the natural convection and radiation losses at the conductor,

the low thermal resistance between conductor and copper clamps influences the measurements, especially on the hot side. The thermal mass of the clamps and feeding cables and their convection and radiation effects are not further evaluated during these experiments. Simplifications have been made to just consider the resistive losses at the conductor and clamp interface creating Joule heating and heat transfer into the coolant. The initial measurements, presented in Table IV, were taken with 100 kPa of pressure difference and water coolant at constant 20 °C.

TABLE IV
MEASURED TEMPERATURES OF THE STRAIGHT PIPE WITH 21 °C−22 °C COOLANT WATER AT CONDUCTOR INLET TP 3 AT A PRESSURE DIFFERENCE OF 100 KPA, LEADING TO A FLOW RATE Q OF ABOUT $0.315\,\mathrm{l/min}$ DURING THE MEASUREMENTS.

Current	TP4	ΔT coolant	TP 1	TP 2	Power
200 A	24.0 °C	2.5 K	23.8 °C	24.1 °C	52 W
300 A	27.2 °C	5.7 K	25.7 °C	28.0 °C	119 W
400 A	31.2 °C	9.7 K	28.7 °C	33.0 °C	213 W
500 A	36.5 °C	15.3 K	32.2 °C	39.6 °C	336 W
520 A	38.8 °C	16.6 K	32.9 °C	41.8 °C	364 W

VI. RESULTS

The simulation results from the mesh independence study are shown in Fig. 6 to indicate the stability of the FEM simulations to the change of mesh density.

A comparison of the measured and analytical calculated pressure drop versus flow rate is provided in Fig. 7. The coolant inlet temperature was kept constantly at 20 °C and no conductor current was applied. For comparison, the FEM simulation result of the W-shaped conductor with a current of 520 A is shown as well. A good match between the analytical turbulent calculation and measured W-shaped conductor was found for the entire measurement range. However, for the straight conductor, the measured pressure drop at flow rates less than $0.18\,\mathrm{l/min}$ is lower compared to the analytical turbulent calculation. It approaches the analytical calculated laminar flow curve. At this flow rate the Reynolds number R_e drops below 2600 so it is assumed that the change from turbulent to laminar flow takes place.

The measurements in Table IV show the coolant and conductor temperature increase at different conductor currents. With a coolant temperature increase of 16.6 K, a good match to the 520 A simulation results shown in Fig. 8 is observed. The measured flow rate Q was found to be slightly larger compared to the measurements taken for Fig. 7. During different measurements with constant pressure, a slight change in flow rate and sudden small temperature changes at different locations along the conductor were observed, especially at the entrance region. Further investigation is required to better understand this phenomena which may lead to minor local conductor temperature rise.

The applied conductor current of 520 A at the simulation leads to a temperature increase and thus alters the coolant

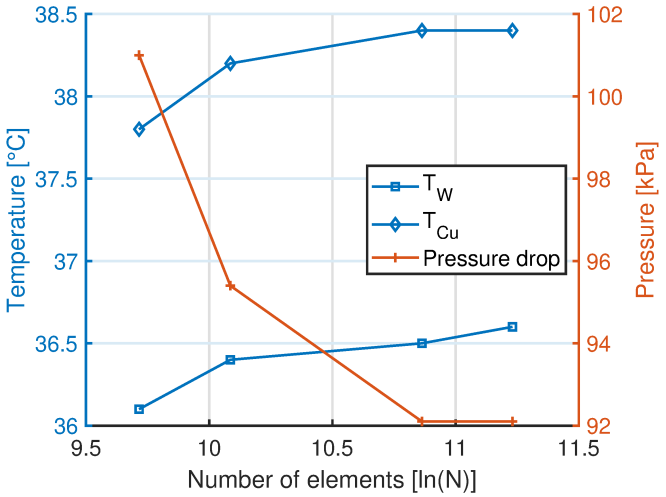

Fig. 6. Temperature of outlet water (T_W), hot end of pipe (T_{Cu}), and pressure drop over the pipe with a constant flow rate of $0.31\,\mathrm{l/min}$

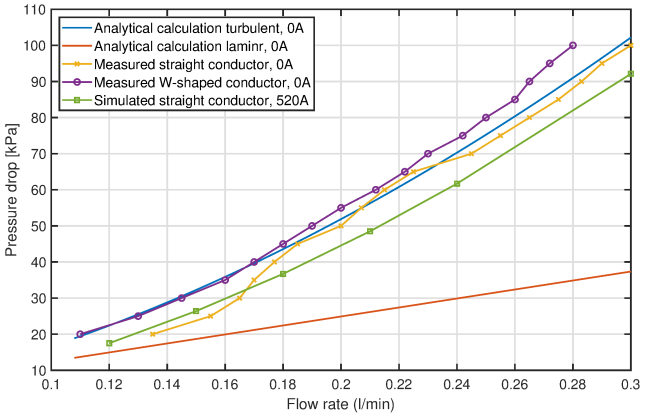

Fig. 7. Measured and analytical pressure drop versus flow rate comparison in both conductor types with a constant coolant inlet temperature of 20 °C and no conductor current. For comparison, the simulated result with 520 A of conductor current.

properties as provided in Table I and Table II. This results in a lower average viscosity of the coolant through the conductor and increased flow at constant pressure and hence increased cooling capacity.

TABLE V
SIMULATED TEMPERATURES OF THE W-SHAPED CONDUCTOR WITH 20°C COOLANT WATER AT THE CONDUCTOR INLET AND A PRESSURE DIFFERENCE OF 100 KPA.

Current	Q	ΔT coolant	$T_{Cu_{MAX}}$
400 A	$0.288\,\mathrm{l/min}$	9.3 °C	31.4 °C
500 A	$0.288\,\mathrm{l/min}$	14.5 °C	37.9 °C
520 A	$0.288\,\mathrm{l/min}$	15.7 °C	39.3 °C

Table V shows the simulated temperature increase of the coolant and maximum conductor temperature reached at different DC currents. The flow rate of the W-shaped conductor is slightly lower compared to the straight version with the coolant

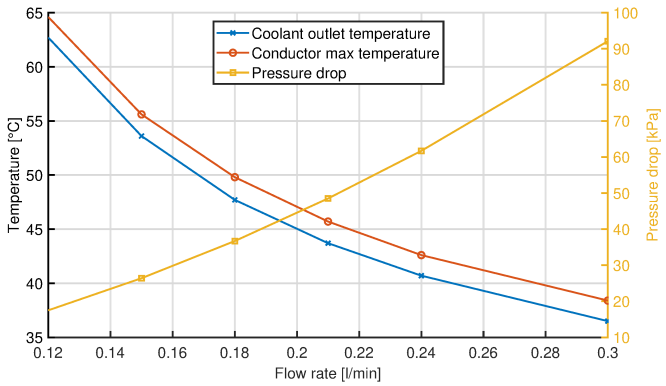

Fig. 8. Simulated temperatures and pressure drop of the straight conductor with 20°C coolant water at the conductor inlet and 520 A current.

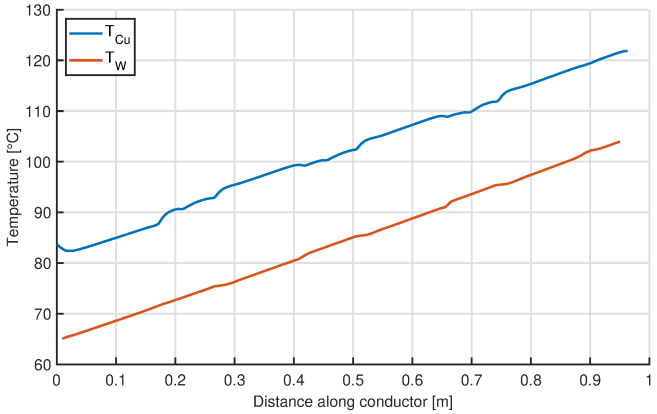

Fig. 9. Temperature distribution along the W-shaped conductor length from the simulation at 700 A with EGW50/50. The blue curve shows the temperature of the conductor wall and the green curve shows the coolant temperature.

water inlet at 20 °C and a pressure difference of 100 kPa.

Fig. 8 shows the temperature rise of coolant and conductor in relation to different coolant flow rates and the adjacent pressure drop that is expected with a coolant water inlet of 20 °C. The simulation of the W-shaped conductor with EGW50/50 coolant at 65°C inlet and 140 kPa gives a flow rate of $Q = 0.312\mathrm{l/min}$, a coolant outlet temperate T_c=104 °C, a maximum copper temperature T_{Cu}=121.9 °C. By using Eq. 7, the pump power required for the complete winding with 48 conductors is $\dot{W} = 70\,\mathrm{W}$.

Fig. 9 shows the temperature along the center line on the outside of the conductor and of the coolant under these

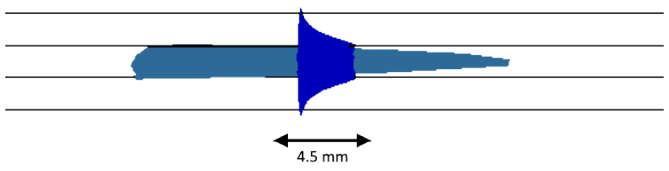

Fig. 10. Iso-surface temperature, the long cone shows a coolant temperature of 93.3°C and short cone shows a conductor temperature of 106.5°C

conditions. It can be observed that the conductor surface temperature and difference to the coolant is reduced at the bends. This is caused by the increased turbulence at the bends, increasing the heat transfer to the coolant.

One representative iso-surface showing the temperature of the conductor and the coolant right after the last bend is shown in Fig. 10. This simulation result justified the assumption used in the analytical calculations of no temperature gradient in the conductor's cross-section.

VII. Conclusion

This paper proposed a novel multi-phase winding used in a 48 V traction drive design, which incorporates in-conductor direct cooling capability. The winding is made with 48 identical preformed hollow copper conductors, shorted together with an end-ring to form a star-topology. Due to the low-voltage nature of the winding design, coolant with better thermal performance such as EGW50/50 can be used to directly cool the entire winding by flowing through the conductors' center. This provides the low-voltage drive design with an important technical advantage in comparison with state-of-the-art high-voltage designs. The latter can only use oil, which has a considerably worse thermal performance, due to the high-voltage insulation requirements. Furthermore, it has to deal with the insulation layer of poor thermal performance, separating the conductor from the coolant.

This paper studied the cooling performance of the hollow copper conductor, both in straight shape and in preformed W-shape, using 20 °C water as coolant, 520 A as load current, a flow rate of about $0.3\,\mathrm{l/min}$ and a pressure drop of about 100 kPa. The study showed that both, the analytical calculation and the FEM simulation results fit well to the experimental results. This good fit indicates an accurate FEM setup.

The results also show that the additional coolant flow rate drop induced by the preformed conductor compared with the straight conductor follows the same trend, at least up to at the pressure of 100 kPa and 20 °C water coolant temperature. Leading to the conclusion that the bends in the conductor do not create much additional flow resistance under these conditions. Furthermore, they help to increase the mixing of the coolant and increase the heat transfer as shown in Fig. 9.

The paper also simulated the cooling performance of the preformed conductor using the same FEM setup in a more demanding scenario, where EGW50/50 coolant of 65 °C inlet temperature is used under a constant load current of 700 A, which translates to a current density of $49.5\,\mathrm{A/mm^2}$. The flow pressure is increased to 140 kPa to accommodate for this scenario. The simulation results showed a power dissipation of 710 W at a coolant flow rate of $0.312\,\mathrm{l/min}$ and an outlet temperature of 104 °C which is below its boiling point of 107.5 °C. The maximum conductor temperature is shown to be only 121.9 °C. From these results, it can be concluded that the preformed copper conductor with the in-conductor direct cooling method proposed here using EGW50/50 coolant can easily handle a current density of at least $50\,\mathrm{A/mm^2}$ and power dissipation of at least 710 W continuously without

reaching its technical limits. This means that, even at a coolant inlet temperature of $65\,^{\circ}\mathrm{C}$, the 48 phase winding can still constantly dissipate at least $34\,\mathrm{kW}$ at a flow rate of about $15\mathrm{l}/\,\mathrm{min}$. Such an exceptional cooling performance will clearly meet the power density requirements of traction drives for future 48 V EV applications.

ACKNOWLEDGMENT

The authors also like to thank Joel Näslin for his support with the measurements.

REFERENCES

[1] X. Chen, J. Wang, A. Griffo, and A. Spagnolo, "Thermal modeling of hollow conductors for direct cooling of electrical machines," *IEEE Transactions on Industrial Electronics*, vol. 67, no. 2, pp. 895–905, Feb 2020.

[2] A. Reinap, F. J. Marquez-Fernandez, M. Alaküla, R. Deodhar, and K. Mishima, "Direct conductor cooling in concentrated windings," in *2018 XIII International Conference on Electrical Machines (ICEM)*, 2018, pp. 2654–2660.

[3] Y. Gai, M. Kimiabeigi, Y. Chuan Chong, J. D. Widmer, X. Deng, M. Popescu, J. Goss, D. A. Staton, and A. Steven, "Cooling of automotive traction motors: Schemes, examples, and computation methods," *IEEE Transactions on Industrial Electronics*, vol. 66, no. 3, pp. 1681–1692, March 2019.

[4] P. Lindh, I. Petrov, A. Jaatinen-Värri, A. Grönman, M. Martinez-Iturralde, M. Satrústegui, and J. Pyrhönen, "Direct liquid cooling method verified with an axial-flux permanent-magnet traction machine prototype," *IEEE Transactions on Industrial Electronics*, vol. 64, no. 8, pp. 6086–6095, 2017.

[5] A. Patzak, F. Bachheibl, A. Baumgardt, G. Dajaku, O. Moros, and D. Gerling, "Iscad - electric high performance drive for individual mobility at extra-low voltages," *SAE International Journal of Alternative Powertrains*, vol. 5, no. 1, pp. 148–156, 2016. [Online]. Available: http://www.jstor.org/stable/26169115

[6] M. Gabassi, "Directly cooled windings - conjugate heat transfer assessment of air-cooled hollow conductor," 2018, student Paper.

[7] M. Schiefer and M. Doppelbauer, "Indirect slot cooling for high-power-density machines with concentrated winding," in *2015 IEEE International Electric Machines Drives Conference (IEMDC)*, May 2015, pp. 1820–1825.

[8] H. Vansompel and P. Sergeant, "Extended end-winding cooling insert for high power density electric machines with concentrated windings," *IEEE Transactions on Energy Conversion*, vol. 35, no. 2, pp. 948–955, June 2020.

[9] N. Sharma and Y. Liu, "Multiple electrical machines applied for high drive train efficiency," in *2018 IEEE International Conference on Electrical Systems for Aircraft, Railway, Ship Propulsion and Road Vehicles International Transportation Electrification Conference (ESARS-ITEC)*, 2018, pp. 1–7.

[10] Fluid properties calculator. Microelectronics Heat Transfer Laboratory, Department of Mechanical Engineering, University of Waterloo, 200 University Avenue West, Waterloo, Ontario, Canada. [Online]. Available: http://www.mhtl.uwaterloo.ca/old/onlinetools/airprop/airprop.html

[11] (2020) Comsol multiphysics® v. 5.3a. www.comsol.com. COMSOL AB. Stockholm, Sweden.

[12] D. Kaya, E. A. Yagmur, K. S. Yigit, F. C. Kilic, A. S. Eren, and C. Celik, "Energy efficiency in pumps," *Energy Conversion and Management*, vol. 49, no. 6, pp. 1662–1673, 2008.

VIII. BIOGRAPHIES

Stefan Haller received his diploma degree in electrical engineering from the University of Applied Sciences, Osnabrueck, Germany in 2009 and his M.Sc degree in electrical engineering from Mid Sweden University, Sundsvall, Sweden in 2010. He is currently working towards his Ph.D. degree in electrical engineering at the Department of Electronics Design at Mid Sweden University. In his research, he is investigating massive multi-phase low-voltage high-current traction machines with integrated MOSFET-based inverters. He has worked with power electronics since 2008 and electrical machines since 2012 and has designed multi-phase high-current machines and converters. His research interests include low-voltage high-current machines, switched mode converters, industrial embedded systems and drives as well as building automation systems.

Johan Persson received the M.Sc. and Ph.D. degrees in engineering physics from Mid Sweden University, Sundsvall, Sweden, in 2010 and 2015, respectively. He is currently a lecturer at the of Department of Natural Sciences at Mid Sweden University. His research interests include mechanical engineering and it's application in forestry and paper making.

Peng Cheng received the M.Sc. and Ph.D. degrees in electrical engineering from Mid Sweden University, Sundsvall, Sweden, in 2006 and 2011, respectively. He is currently a researcher at the Department of Electronics Design at Mid Sweden University. His research interests include low-voltage electric drives and industrial sensor design and application.

Kent Bertilsson received the M.Sc. degree in electronics from Mid Sweden University, Sundsvall, Sweden, in 1999, and the Ph.D. degree in the field of device design and optimization of silicon carbide devices from the Royal Institute of Technology, Stockholm, Sweden, in 2005. Since 2005, he is leading the research in power electronics at Mid Sweden University, where he is currently a Full Professor. In 2009, he co-founded SEPS Technologies AB, Sundsvall, where he is also the CEO. He has authored or coauthored more than 60 articles in international journals and conferences in the fields of semiconductor device simulations, silicon carbide devices, detectors, and power electronics.